Applied Catalysis B: Environmental 148–149 (2014) 473–483

Contents lists available at ScienceDirect

Applied Catalysis B: Environmental

journal homepage: www.elsevier.com/locate/apcatb

Abatement of Acid Orange 7 in macro and micro reactors. Effect of the electrocatalytic route

Onofrio Scialdone*, Alessandro Galia, Simona Sabatino

Dipartimento di Ingegneria Chimica, Gestionale, Informatica, Meccanica, Università degli Studi di Palermo, Viale delle Scienze, 90128 Palermo, Italy

ARTICLE INFO

Article history:
Received 11 August 2013
Received in revised form 29 October 2013
Accepted 4 November 2013
Available online 25 November 2013

Keywords:
Electrocatalysis
Micro reactor
Active chlorine
Electro-Fenton
BDD
Acid Orange 7

ABSTRACT

The electrochemical treatment of aqueous solutions contaminated by Acid Orange 7 (AO7) was widely studied with the main objective to evaluate as the electrocatalytic route affects the performances of the degradation process in macro and microfluidic cells. Direct anodic oxidation (EO), electro-Fenton (EF), electro-generation of active chlorine (IOAC) and coupled processes were investigated in macro and microfluidic reactors in order to select more effective conditions for the treatment of such compound. The effect of numerous operative parameters (such as nature of the electrode materials, coupling of processes, flow rate, current density and inter-electrode distance) on the performances of the process was studied in detail. It was found that the catalytic route affects strongly the performances of the process in terms of removal of color, abatement of AO7 and COD and nature of by-products. Furthermore, different operative conditions were required to optimize the various electrocatalytic routes. The utilization of micro devices allowed to work without the addition of a supporting electrolyte and improved the performances of EO and EF that are kinetically controlled by mass transfer processes. On the other hand, the performances of IOAC did not depend on the adopted reactor.

1. Introduction

Very large amounts of synthetic dyes are discharged in the environment from industrial effluents [1]. A loss of 1–2% in production and 1–10% in use are estimated. Due to their large-scale production and extensive application, synthetic dyes can cause considerable nonaesthetic pollution and are serious health-risk factors [2]. Dyes are commonly classified from their chromophore group. The majority of these compounds consumed at industrial scale are azo (—N=N—) derivatives that represent more than 50% of the all dyes used in textile industries, although antraquinone, indigoide, triphenylmethyl, xanthene, sulfur and phtalocyanine derivatives are frequently utilized [3].

Since dyes usually present high stability under sunlight and resistance to microbial attack and temperature, most of these compounds are not degradable in conventional wastewater treatment plants. The research of powerful and practical treatments to decolorize and degrade dyeing wastewaters to decrease their environmental impact has then attracted increasing interest over the past two decades. Electrochemical methods are considered to be among the more efficient Advanced Oxidation Processes (AOPs) for the removal of dyes [2]. The main electrochemical procedures utilized for the remediation of dyestuffs wastewaters are electrocoagulation (EC), direct electrochemical oxidation (EO) with different anodes, indirect electro-oxidation with active chlorine (IOAC) and Electro-Fenton (EF) [2]. The azo dye Acid Orange 7 (AO7), also called Orange II ($C_{16}H_{11}N_2NaO_4S$), was often chosen as model compound to evaluate promising approaches because, being a simple molecule, it is very useful as test and since it is widely used in paperboard industries, for coloration, and in wool textile dyeing.

The electrochemical oxidation of aqueous solutions of AO7 was previously investigated by various authors [4–10]. Fernandes et al. studied the electrochemical oxidation at BDD anodes both in the absence and in the presence of chlorides. An almost complete colour removal and very high COD removal were obtained. In the presence of KCl a faster colour removal was achieved as a consequence of active chlorine formation [4]. A detailed study on the effect of the supporting electrolyte on the oxidation of AO7 at BDD anode was carried out by Zhang et al. [6]. Peralta-Hernandez et al. compared the performances of hydrogen peroxide based processes (direct photolysis, electro-Fenton process and photoelectro-Fenton process) [7]. Electro-Fenton process (EF) was, in particular, studied in detail by various authors [7–10]. Oturan and co-authors studied in detail the nature of intermediates and by-products [8]. Garcia-Segura et al. [10] studied the abatement of monoazo, diazo and triazo dyes by EF in the presence of a gas diffusion cathode and a BDD anode.

* Corresponding author. Tel.: +39 09123863754; fax: +39 09123860841.
E-mail address: onofrio.scialdone@unipa.it (O. Scialdone).

0926-3373/$ – see front matter © 2013 Elsevier B.V. All rights reserved.
http://dx.doi.org/10.1016/j.apcatb.2013.11.005

According to the literature, the performances of the electrochemical treatment of dyes are likely to strongly depend on the adopted electrocatalytic route [2]. However, in spite of the numerous papers devoted to the electrochemical treatment of azo dyes, comparisons of various electrocatalytic routes under similar and optimized operative conditions were not usually carried out. In this paper, the possible utilization of more promising electrocatalytic routes for the treatment of aqueous solutions of Acid Orange 7 chosen as a model compound (namely, direct electrochemical oxidation, indirect oxidation with active chlorine and electro-Fenton) used alone or in a combined way was widely and systematically studied to evaluate as the electrocatalytic route affects the degradation process. Both conventional cells and microfluidic apparatus were used in order to select more effective electrochemical conditions for the treatment of such compound.

Thus, recently it has been demonstrated that the electrochemical abatement of organic pollutants in water by both anodic direct oxidation and electro-Fenton process can strongly benefit from the utilization of microfluidic electrochemical reactors (i.e. cells with a distance between the cathode and the anode of tens or hundreds of micrometers) [11–13]. Very small distances between electrodes lead from one side to a drastic reduction of ohmic resistances [11–14] (allowing to operate with lower cell voltages and without supporting electrolyte) and on the other side to increase the abatement of organic pollutants [12,13]. These aspects are of particular relevance for the treatment of dyes. Indeed, real textile effluents often present quite low conductibility that imposes the addition of a costly supporting electrolyte [15] or the utilization of a microfluidic reactor to achieve reasonable cell voltages. In this paper a systematic comparison between conventional cell and micro reactors for various electrocatalytic route (namely, direct anodic oxidation, electro-Fenton, oxidation by electrogenerated active chlorine) and coupled approach was carried out for the first tine.

The effect of numerous operative parameters, including the nature of the electrode materials, flow rate, current density, and the inter-electrode distance, on the performances of the process was also systematically studied to determine more proper operative conditions.

2. Experimental

2.1. Electrolyses

Electrolyses in macro-scale were performed in batch mode in a cylindrical, undivided tank glass cell under vigorous stirring performed by a magnetic stirrer with 50 mL of solution. For EF experiments, compressed air was fed (0.35 L min^{-1}) to the water solution by a diffuser or directly inside the Air Diffusion Electrode (ADE). The inter-electrode gap was about 2 cm. Experiments in the micro reactor were performed in a continuous mode with a single passage of the solution inside the cell using a syringe pump (New Era Pump Systems, Inc.) to feed the solutions with flow rate between 0.05 and 0.4 mL/min and without addition of a gaseous stream to the solution. The micro reactor consists in a commercial undivided filter press flow cell ElectroCell AB, equipped with one or more polytetrafluoroethylene (PTFE) spacers with the following nominal distances between electrodes: 50 (using one spacer), 75 (using two spacers of 50 and 25 μm), 120 (with a single spacer) and 240 μm (using two spacers of 120 μm). Spacers were cut to define the working surface ($A = 5\ cm^2$). For each tested operative condition at least 3 samples of 1 mL were analyzed to be sure that steady state conditions were achieved.

Electrolyses were driven by an Amel 2053 potentiostat/galvanostat operated in galvanostatic mode. Electrolyses were usually performed at room temperature with an initial AO7 concentration of 0.43 mM. Na_2SO_4 (0.035 M) was used as supporting electrolyte for experiments carried out in the macro device. $FeSO_4$ (0.5 mM) was used as catalyst for EF processes.

2.2. Analyses

The concentration of H_2O_2 was determined from the light absorption of the Ti(IV)—H_2O_2 colored complex at $\lambda = 409$ nm, using $O_5STi{\cdot}H_2SO_4$ from Fluka. The chemical oxygen demand (COD), a routinely measure that determines the quantity of oxygen required to oxidize the organic matter in a sample, under specific conditions of oxidizing agent, temperature and time, was evaluated using Merck cell tests. The removal of color was monitored from the decay of the absorbance (A) at $\lambda = 482$ nm for AO7 [10]. An Avantes Optic Spectrophotometer (DH-2000) was used. The total organic carbon (TOC) was analyzed by a TOC analyzer Shimadzu VCSN ASI TOC-5000 A. The degradation of AO7 and of some byproducts was monitored by high-performance liquid chromatography (HPLC) using a Hewlett Packard 1100 system, equipped with UV–vis detector, and fitted with a Platinum EPS C18 column 100A 5 μ, 4.6 mm × 250 mm, from Alltech, which was thermostated at 25 °C. Injection volumes were 30 μL. The column was eluted at isocratic mode with a mixture of a buffer solution, containing HK_2PO_4 (99 + % ACS reagents, Aldrich) and H_3PO_4 at pH 2.5, methanol (≥99.9% for HPLC, Aldrich), 1-pentanol (ACS reagent, ≥99%, Aldrich), 65:30:5 (v/v) with a flow rate of 1 mL min^{-1}. Detection was performed at 280 nm.

Carboxylic acids were identified and quantified using the same system by a Preavail Organic Acid 5 μ column, 4.6 mm × 250 mm, from Grace with a 100% of the same buffer solution. The detection was performed at 210 nm with a flow rate of 1 mL min^{-1}. Calibration curves were obtained by using the pure standards of the related carboxylic acids. The eventual presence of chlorinated products was evaluated by HPLC/MS thermo TSQ Quantum Access, Type ESI, negative Polarity Q1 MS, fitted with a Zic-Hilic column 5 μ, 2.1 mm × 150 mm, from Merck. The column was eluted with a mixture of a buffer solution, containing CH_3CN (99+% ACS reagents, Fluka) and 10 mM of Ammonium Acetate (99+% ACS reagents, Aldrich) at pH 5, 90:10 (v/v).

The thickness of the stagnant layer in the adopted conditions was estimated trough a typical limiting-current essay using the redox couple hexacyanoferrate(II)/hexacyanoferrate(III) focusing on the oxidation reaction and using the value $6.631 \times 10^{-10}\ m^2\ s^{-1}$ for the diffusivity of ferry-cyanide ion [16]. The mass transfer coefficient of AO7 k_m was estimated as the ratio between its diffusivity D (assumed to be about $10^{-9}\ m^2\ s^{-1}$) and the thickness of the stagnant layer.

The color removal X was computed by Eq. (1) [10] while the current efficiency CE for the removal of COD was defined by Eqs. (2) and (3) [11,13] for a macro and a micro cell, respectively.

$$\text{Color removal} = \frac{(A^0 - A^f)}{A^0} \tag{1}$$

$$CE = \frac{nFVCOD^0X}{(i_{app}At)} \tag{2}$$

$$CE = \frac{nFCOD^0X\Phi_V}{(i_{app}A)} \tag{3}$$

where A° and A^f are the absorbance at initial time and time t at $\lambda = 482$ nm, n is the number of electrons, F the Faraday constant (96487 C mol^{-1}), i_{app} the applied current density, V the volume of the cell and Φ_V the volumetric flow rate. Similarly, for generation of H_2O_2 in micro-device, $CE = 2F[H_2O_2]\Phi_V/(i_{app}A)$.

2.3. Materials

Bi-distilled water and Acid Orange 7 (Sigma–Aldrich) were used as solvent and model pollutant, respectively. Na_2SO_4 35 mM (Janssen Chimica) was used as supporting electrolyte for experiments in macro cell and $FeSO_4$ (Fluka) 0.25–1 mM as catalyst for EF. H_2SO_4 was used to have a pH of 3 for EF processes. Main by-products were determined by HPLC analyses by comparison of their retention times with that of pure standards. Oxalic (Sigma–Aldrich), formic (Sigma–Aldrich), tartaric (Merck), malonic (Alfa Aesar), acetic (Sigma–Aldrich), salicylic (Merck), maleic (Merck), succinic (Fluka), fumaric (Fluka), lactic (Sigma–Aldrich), and phtalic (Fluka) acids, hydroquinone (Sigma–Aldrich), 1,2-naphthaquinone (Sigma–Aldrich), and 4-amminophenol (Sigma–Aldrich), were used as standards for HPLC analyses. Compact graphite (Carbon Lorraine), carbon felt (The Electosynthesis Co.), a carbon-PTFE ADE from E-TEK, which was fed with 0.35 L min^{-1} of compressed air to electrogenerate H_2O_2, or Ni were used as cathodes while $Ti/IrO_2–Ta_2O_5$, $Ti/RuO_2–IrO_2$ and BDD-Nb, supplied by ElecroCell AB, were used as anodes with a geometric surface of 5–6 cm^2. Prior to each experiment, diamond electrodes were polarized at 3.0 V vs. SCE for 5 min.

3. Results and discussion

The abatement of AO7 by various electrocatalytic routes (direct anodic oxidation, electro-Fenton, oxidation by electro-generated active chlorine) was widely investigated by a large series of experiments. First, each catalytic route was investigated in detail with the main objective to evaluate the effect of the microreactor and of other operative parameters on the process (Sections 3.1–3.3). After, a comparison between the electrocatalytic routes was performed (Section 3.4) while the last part of the study was devoted to the investigation of coupled approaches (Section 3.5).

3.1. Direct electrochemical oxidation

The direct anodic oxidation of organic pollutants (EO) has been extensively investigated in the last years. It was shown that EO can present higher abatements with limited costs with respect to ozonation and Fenton oxidation processes [17]. The performances of the process in terms of complete mineralization of organic pollutant and current efficiency depends dramatically on the nature of the anode [18,19]. A high number of electrodes have been tested for the treatment of dyes including metal oxides, carbonaceous materials, Pt and PbO_2 [18]. However, synthetic BDD thin films are currently preferred as anodes due to their high performances [20]. The electrochemical oxidation of AO7 was previously carried out at commercial BDD in undivided conventional cells [4,6]. Zhang et al. [6] have shown that the process is affected by both applied current density and nature of electrolyte cation. Here the direct electrochemical oxidation of AO7 was performed in conventional cells equipped with magnetic stirring and in micro reactors with a distance between the electrodes of about 50 μm. Both BDD and

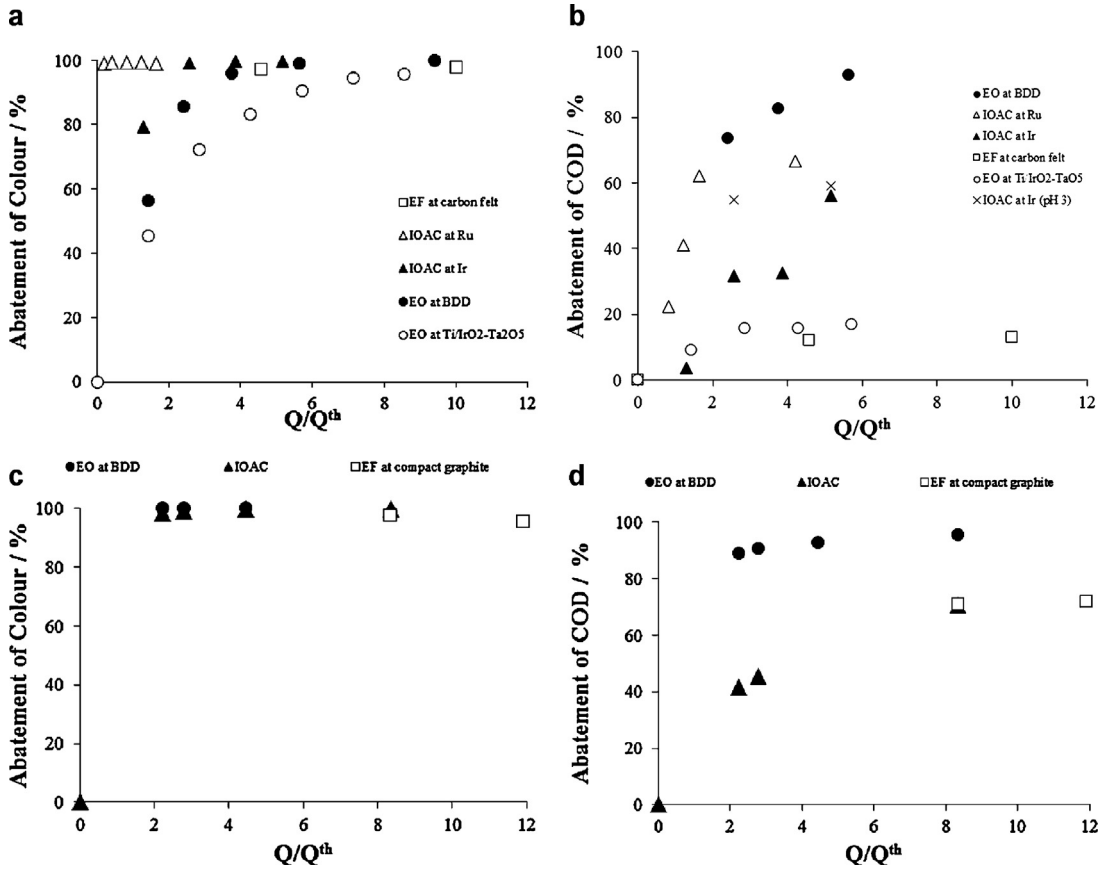

Fig. 1. Plot of colour (a and c) and COD abatement (b and d) vs. dimensionless passed charge (the ratio charge passed/theoretical charge) Q/Qth for the electrochemical treatment of a water solution of AO7 in a conventional (a and b) and micro cell (c and d). The electrochemical oxidation was performed by direct anodic oxidation at $Ti/IrO_2–Ta_2O_5$ (o) and BDD anode (●), indirect oxidation by means of electrogenerated active chlorine at $Ti/IrO_2–Ta_2O_5$ (initial pH 7▲, initial pH 3x) and $Ti/RuO_2–IrO_2$ (△) anode with 17 mM of NaCl and electro-Fenton (pH 3 □). Current density: 20 A/m^2 for electro-Fenton in micro device, 100 A/m^2 for other experiments. Cathode for EO and indirect oxidation by active chlorine: nickel. Cathode for electro-Fenton: carbon felt for conventional cell and compact graphite for micro device. Anode for electro-Fenton: Ti/IrO_2-Ta_2O_5. Nominal distance between the electrodes in the micro reactor 50 μm for EO and IOAC and 120 μm for EF. Flow rate in the micro reactor: 0.1–0.4 mL/min. Theoretical charge Qth is the charge necessary to mineralize all the initial COD with a process with a current efficiency of 100%.

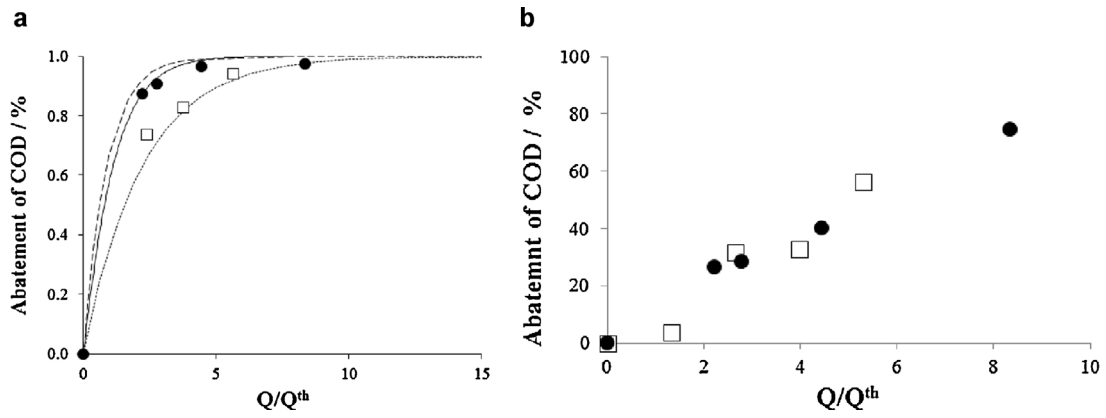

Fig. 2. Trend of abatement of COD vs. *Q*/Qth for the electrochemical oxidation of AO7 by direct oxidation at BDD (a), electrogenerated active chlorine at Ti/IrO_2–Ta_2O_5 with 17 mM of NaCl (b) in conventional cell (□) and in the micro reactor (●) at 100 A/m^2. Cathode: Nickel. Nominal distance between the electrodes in the micro reactor 50 μm. Flow rate in the micro reactor: 0.1–0.4 mL/min. Figure a reports also the theoretical predictions for a process under mass transfer control in a conventional cell (. . .) and in a microfluidic reactor (- -) and for a process under a mixed kinetic regime in a micro fluidic reactor (—) computed according to literature [12] (see Appendix A).

Ti/IrO_2–Ta_2O_5 were used as anodes. In both cases, the process was performed at high anodic voltages necessary to allow the oxidation of water, thus maintaining the anode activity. As shown in Fig. 1a, a drastically higher color removal was obtained at BDD anodes with respect to that achieved at iridium based anode. This is due to the fact that at BDD, very reactive free or loosely adsorbed hydroxyl radicals are formed (Eq. (4)) which have a strong oxidation power. In the presence of low organic concentrations as usually occurs with the treatment of pollutants, the oxidation at BDD occurs under the kinetic control of the mass transfer of the pollutant to the anode surface [21]. Under adopted operative conditions, the applied current density *i* was higher than the limiting current density expected for a process under a mass transfer control $i_{lim} = nFk_mC_{AO7}$ (where *n* is the number of electrons necessary for the oxidation of the pollutant to carbon dioxide and k_m and C_{AO7} are the mass transfer coefficient and the bulk concentration of AO7) for almost all the process (initial $i_{lim} = 55$ A/m^2 < $i = 100$ A/m^2). As shown in Fig. 2a, the abatement of COD at the BDD anode was very similar to that theoretically expected for a process under mass transfer kinetic control obtained by using a simple theoretical model developed by some of the authors [12,21,22] (see Appendix A). The lower abatement achieved at iridium based anodes is due to the fact that the oxidation of water results in the formation of chemisorbed oxygen (Eqs. (5) and (6)) that have a less oxidation power and that gives rise more easily to the competitive oxygen evolution (Eq. (7)) [12,22,23].

$$BDD + H_2O \rightarrow BDD(^{\bullet}OH) + H^+ + e^- \quad (4)$$

$$MO_x + H_2O \rightarrow MO_x(^{\bullet}OH) + H^+ + e^- \quad (5)$$

$$MO_x(^{\bullet}OH) \rightarrow MO_{x+1} + H^+ + e^- \quad (6)$$

$$MO_{x+1} \rightarrow MO_x + 0.5O_2 \quad (7)$$

According to above considerations, the performances of the process at BDD anode are expected to depend mainly on the flow-dynamic conditions. Hence, experiments were repeated in a micro reactor that offers the advantage of fast mass transport kinetics, lower cell voltages and the possibility of working in the absence of supporting electrolytes also in water solutions with low conductivity as it can happen for discharged waters from textile dyeing industry [15]. Higher abatements were achieved in the micro cell for the same amount of charge passed, as a result of the fast mass transport, with respect to that recorded in the conventional cell (Fig. 2a).

Increasing the flow rate (i.e., lowering the treatment time) one has lower abatements (Fig. 3) but higher current efficiencies (data not shown) and productivity of the cell. In this perspective, the flow rate and as a consequence the productivity of the cell can be properly selected for each target abatement for a given geometry of the microcell. Higher current efficiencies but lower abatements can be obtained also reducing the current density (Fig. 3). In this case the process is no longer under a pure kinetic control of the mass transport of the organics to the anode surface and a more complete theoretical model has to be adopted to describe the experimental results. Here we used a simple model developed by some of the authors [12] and briefly reported in Appendix A. As shown in Figs. 2 and 3, data were well fitted by theoretical predictions. The model involves a fitting parameter named $[RH]^*$ that is defined as the concentration of the organic which gives a current efficiency of 50% in the absence of mass transfer limitations, e.g., the concentration of the organic *RH* at the anode surface $[RH]_x^{y=0}$ which gives a current density for the *RH* mineralization equal to the current density involved for the oxygen evolution reaction [12]. Of course, the higher is the value of $[RH]^*$ more favored is the oxygen evolution

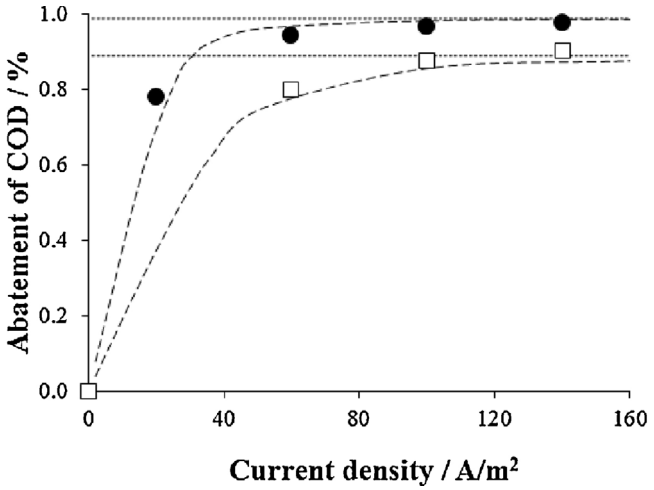

Fig. 3. Direct electrochemical oxidation of AO7 at BDD anode in the micro reactor. Effect of current density on the abatement of COD at 0.2 (●) and 0.4 (□) mL/min. Nominal distance between the electrodes 50 μm. Cathode: nickel. Theoretical curves are the predictions for a process under mass transfer control (. . .) and under mixed kinetic regime (- -) computed according to literature [12] (see Appendix A).

while the lower is $[RH]^*$ more favored is the mineralization of the organic. Hence, the fitted value of $[RH]^*$ can be used to evaluate the mineralization power of an anode for a selected organic pollutant. In our case a fitting value of $[RH]^*$ of about 3×10^{-2} mM was obtained which confirms that BDD anodes are very suitable for the mineralization of AO7.

HPLC analyses showed that the abatement of AO7 gave rise to the formation of very few by-products (namely, oxalic and formic acids) that were however mineralized at longer times. Indeed, it has been shown in literature that carboxylic acids such as oxalic, formic and maleic acids are usually the main intermediates formed during the oxidation at BDD anodes of more complex substrates such as aromatic ones [38].

3.2. Oxidation by electro-generated active chlorine

Aqueous solutions of organic pollutants can be decontaminated by indirect oxidation with electro-generated active chlorine (IOAC), where anodic oxidation of chloride ions leads to the formation of free chlorine, hypochlorous acid and/or hypochlorite, depending on the pH (Eqs. (8)-(10)), that can oxidize the organics near to the anode or/and in the bulk of the solution (Eq. (11) in alkaline medium) [24–26].

$$Cl^- = Cl_2 + 2e^- \quad (8)$$

$$Cl_2 + H_2O = HOCl + H^+ + Cl^- \quad (9)$$

$$HOCl = H^+ + OCl^- \quad (10)$$

$$\text{Organics} + OCl^- \rightarrow \text{intermediates} \rightarrow CO_2 + Cl^- + H_2O \quad (11)$$

These reactions take place in competition with oxygen evolution, chlorate chemical and electrochemical formation and reduction of oxidants in the presence of undivided cells [25–28]. To account for some experimental results and in particular for the different distribution of byproducts observed in the electrochemical treatment in the presence of Cl^- and in the chemical oxidation with NaClO [25,29], some authors have suggested that an important role can be played also by surface electrochemical reactions. In particular, it has been proposed [29,30] that adsorbed chloro- and oxychloro-radicals could be involved in the oxidation mechanism (see as an example Eqs. (12) and (13) for the oxychlroradicals).

$$MO_x(OH) + Cl^- \rightarrow MO_x(HOCl) + e^- \quad (12)$$

$$\text{Organics} + MO_x(HOCl) \rightarrow \text{intermediates} \rightarrow MO_x + CO_2 + Cl^- + H_2O + H^+ \quad (13)$$

This method allows to avoid the transport and storage of dangerous chlorine, gives faster destruction of organic matter and lower costs than in chemical oxidation. On the other hand, the formation of undesirable toxic chloro-organic derivatives such as chloroform and of chlorine–oxygen by-products such as ClO_2, ClO_3 and ClO_4 can occur. The electrochemical oxidation of numerous dyes with active chlorine in aqueous solutions was studied by various authors [2]. DSA-type anodes (metal oxides supported on Ti) were mainly used due to the high generation of active chlorine expected at these anodes [24,27]. BDD anodes are often not used in the presence of high concentrations of chlorides due to their low efficacy for the conversion of chlorides to active chlorine [24] and for the possible generation of chlorates and perchlorates [31–33]. In the presence of DSA, high color removal was always observed while the removal of COD strongly depended on the investigated system [2]. However, data available in literature on the utilization of IOAC for the treatment of aqueous solutions of AO7 were mainly based on the utilization of a BDD anode [4].

To evaluate the electrochemical oxidation of AO7 with active chlorine, first experiments were here carried out at $Ti/IrO_2–Ta_2O_5$ and $Ti/RuO_2–IrO_2$ anodes that are characterized by a quite low overpotential for oxygen and chlorine, respectively, in the presence of 17 mM of NaCl (initial pH close to 7). Thus, Ir and Ru based anodes gives very low removal of the color by direct EO (see Section 3.1) but high current efficiency for the oxidation of chloride ion to active chlorine (data not shown and reference [24]). A very high abatement of color (Fig. 1a) and AO7 (data not shown) was achieved at both electrodes, thus showing that active chlorine can be effectively used to oxidize this azoic dye and to remove the color or the solution. A slower abatement of COD occurred (Fig. 1b). In particular a higher abatement of COD was obtained at Ruthenium based electrodes as a result of the fact that this electrode is expected to generate an higher amount of active chlorine [24]. On the other hand, a less removal of COD was observed in the experiments performed with electro-generated active chlorine with respect to EO at BDD anode (Fig. 1b). Furthermore, the formation of a colored precipitate was observed during the electrolysis carried out at Iridium based anodes. Since, the oxidation power of active chlorine can depend on the pH oxidation [24], the experiment at iridium cathode was repeated at a pH of 3. As shown in Fig. 1b, a slightly higher abatement of AO7 was obtained (59% vs. 54% after 5.2 Q/Qth) by using a more acidic pH. Hence, it is possible to conclude that electrogenerated active chlorine is very active for the oxidation of AO7 and for de-colorization purposes but less for its mineralization due to the formation of organic intermediates that present a higher resistance to the oxidation by means of active chlorine. In particular, as mentioned in detail in the following, numerous byproducts were detected, the main relevant being hydroquinone and oxalic, lactic and malonic acids. No chlorinated hydrocarbons were however detected. The latter is a very relevant point since the possible formation of chlorinated organics is considered the main disadvantage given by IOAC processes.

A second series of experiments was carried out in microfluidic devices. It was the first study devoted to the utilization of electro generated active chlorine for the abatement of organic pollutants in water in microfluidic devices. Very similar abatements of both color (data not shown) and COD (Fig. 2b) were obtained in conventional cells and in microfluidic reactors, thus showing that the oxidation process takes place mainly in the bulk of the solution and that eventual surface processes (as that reported in Eqs. (12)–(13)) are not limited by mass transfer kinetics. To evaluate the effect of residence time and current density on the performances of the process, a series of experiments was performed in the micro-fluidic cell by changing both the current density and the flow rate. As shown in Fig. 4, the abatement of both color and COD decreased with the flow rate (e.g., lowering the residence time) and increased with the current density. According with the literature, the increase in the current density results in higher bulk concentrations of active chlorine that allow an higher abatement of COD for the same time of contact (e.g., for the same flow rate). Quite interestingly, a drastic effect of current density was observed for the higher values of the flow rate while similar abatements were observed by changing the current density for experiments performed at 0.1 mL/min. This should indicate that for high enough residence times, the concentration of active chlorine is no longer the limiting factor for the abatement of COD.

3.3. Oxidation by electro-Fenton process

Electro-Fenton process (EF) is based on the electro-generation of hydrogen peroxide in aqueous solution by two-electron reduction

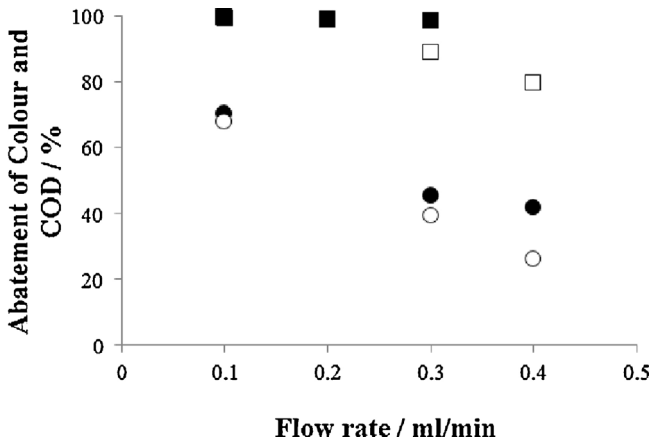

Fig. 4. Oxidation of AO7 by electrogenerated active chlorine in the micro reactor. Effect of flow rate on the abatement of colour (□ 60, ■ 100 A/m^2) and COD (○ 60, ● 100 A/m^2). Nominal distance between the electrodes 50 μm. Anode: Ti/IrO_2–Ta_2O_5. Cathode: nickel. Initial concentration of NaCl 17 mM.

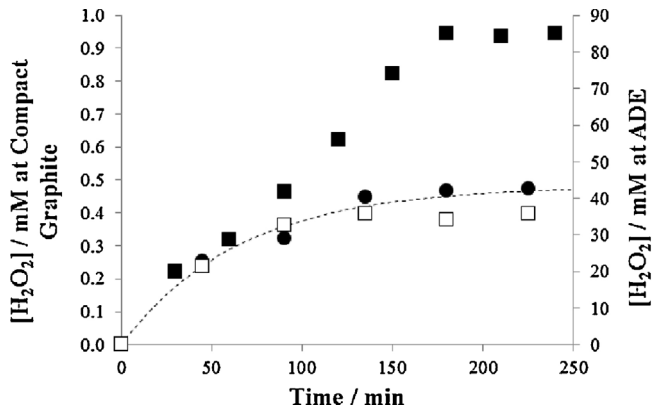

Fig. 5. Evolution of the concentration of H_2O_2 accumulated during the electrolysis of 50 mL of 35 mM Na_2SO_4 solutions of pH 3.0 at 25 °C using a conventional undivided tank glass cell equipped with graphite (●) or ADE (■) cathode and a Ti/IrO_2–Ta_2O_5 anode at 500 A/m^2. Some experiments were repeated with Fe(SO_4) (0.5 mM) at ADE cathode (□).Theoretical curve are the predictions for a process of reduction of oxygen to hydrogen peroxide under kinetic mass transfer control (. . .).

of dissolved oxygen (Eq. (14)) on a cathode such as mercury pool, compact graphite, carbon felt, activated carbon fiber and carbon-polytetrafluoroethylene-O_2 diffusion cathode (ADE) [2,34]:

$$O_2 + 2H^+ + 2e^- \rightarrow H_2O_2 \quad (14)$$

$$H_2O_2 + Fe^{2+} \rightarrow Fe^{3+} + OH^\bullet + OH^- \quad (15)$$

The oxidizing power of H_2O_2 is enhanced in the presence of Fe^{2+} via classical Fenton's reaction (Eq. (15)) which leads to the production of hydroxyl radicals. Reaction (15) is propagated through the continuous electro-generation of Fe^{2+} by reduction of Fe^{3+} by Reaction (16).

$$Fe^{3+} + e^- \rightarrow Fe^{2+} \quad (16)$$

It has been shown that the performances of EF process strongly depend on both cathode and anode materials [39]. The abatement of AO7 in water by EF processes was studied by various authors [7–10]. According to literature [10], the addition of 5 mmol dm^{-3} H_2O_2 to AO7 solution did not cause a relevant removal of color. The color removal at ADE was very poor in the absence of iron but quite quick in the presence of 0.5 mM Fe^{2+} [10]. At compact graphite cathodes the removal of COD was quite slow in macro-device but drastically accelerated in micro-ones [13]. Oturan and co-authors studied the EF process at carbon felt cathodes [8]. Identification of main intermediates was achieved, thus allowing to propose a plausible mineralization pathway [8]. Malonic, formic, acetic and glioxylic acids and various aromatic products such as hydroquinone, 1,2-naphtaquinone, 4-amminiphenol and 4-amminobenzenesulfonic acid were found as by-products [8].

Since the EF treatment is based on the H_2O_2 electro-generation for the •OH production from Fenton's reaction, a first trial of experiments was carried out to evaluate the production of H_2O_2 in adopted systems. Fig. 5 shows the time course of this species during the electrolysis of water solutions in the absence of Fe^{2+} and organics at compact graphite and ADE cathodes in conventional cells. In all cases H_2O_2 was gradually accumulated during the first 240 min, reaching a steady value that depended dramatically on adopted electrode. Hydrogen peroxide is consumed by electrochemical reduction at the cathode surface, disproportion in the bulk and, for undivided cells that are often used to avoid the voltage penalty of the separator, oxidation to oxygen at the anode (Eq. (17)) [35]. Consequently the accumulation of H_2O_2 is lower than its electro-generation.

$$H_2O_2 \rightarrow O_2 + 2H^+ + 2e^- \quad (17)$$

At both graphite (Fig. 5) and carbon felt (data not shown), according to literature [9,38], a steady value lower than 1 mM was reached as a result of the low solubility of oxygen in water (about 40 or 8 mg L^{-1} at 1 atm and 25 °C for pure oxygen or air, respectively, [35]) that imposes a slow mass transfer of oxygen to the cathode surface (see theoretical predictions in Fig. 5). In the case of the ADE, according to literature very high steady values slightly lower than 100 mM were observed as a result of the dramatic enhancement of kinetics of the cathode process which no longer suffers from mass transfer limitations in the liquid phase [36]. When experiments were repeated at ADE cathode in the presence of iron (II) a lower concentration of hydrogen peroxide was detected as a result of the reaction between Fe(II) and H_2O_2 (Eq. (15)).

The generation of hydrogen peroxide in a micro cell equipped with a graphite electrode in the absence of added air was recently studied by the authors [13]. At the best adopted operative conditions (i close to 20–60 A/m^2, inter-electrodic distance h = 120 μm), the reduction of electro-generated oxygen in the microdevice gave rise to a concentration of H_2O_2 of about 6 mM, one order of magnitude higher than that achieved in conventional cells equipped with the same graphite cathode [13].

When electrolyses were performed with both Fe(II) and AO7, the abatement of color was quite fast and similar at all adopted electrodes (carbon felt, compact graphite, ADE) both in conventional and microfluidic cell (Fig. 6a) even if not complete. On the other hand, the abatement of TOC (Fig. 6b) depended strongly on both adopted cathode and electrochemical cell. Higher abatements of TOC were achieved in the micro reactor equipped with compact graphite with respect to that achieved in the conventional cell equipped with ADE, carbon felt or compact graphite, for the same amount or the ratio Q/Qth (Fig. 6b). In the conventional cell, the higher abatements were achieved at ADE and the lower ones at compact graphite, as a result of the low generation of hydrogen peroxide recorded on this electrode. Also carbon felt gave higher abatements than compact graphite. According to literature, at carbon felt and ADE cathodes Fe(II) and Fe(III) dominate, respectively [40]. Hence, at carbon felt a lower formation of Fe(III)-carboxylic acids complexes very resistant to the mineralization is expected [40] while at ADE an higher formation of hydrogen peroxide occurs.

According to literature [13], the utilization of microfluidic cell equipped with compact graphite allowed to increase dramatically the abatement of TOC (Fig. 6b) and AO7 (Fig. 7e) with respect to that achieved in the conventional cell equipped with the same graphite cathode. The higher abatement of TOC and AO7 achieved in the

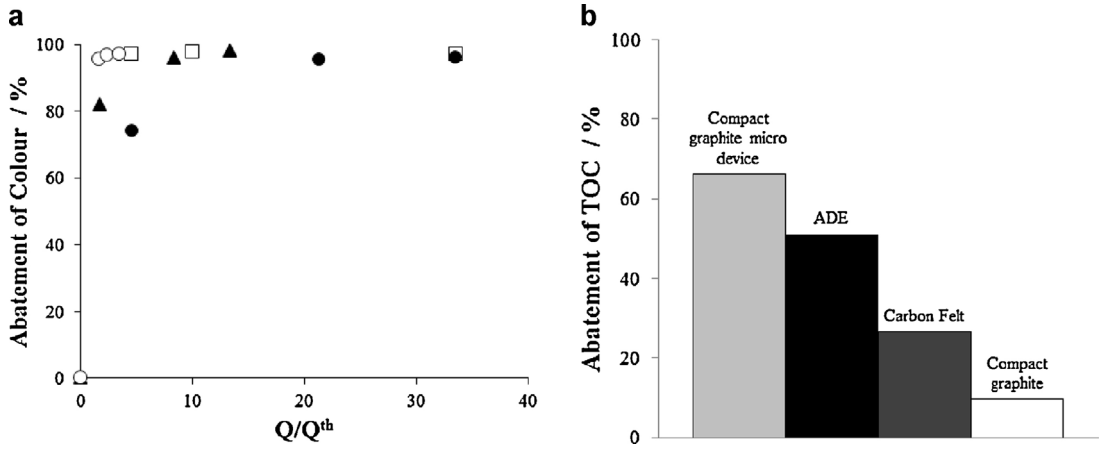

Fig. 6. Abatement of colour vs. Q/Qth (a) for a solution of 50 mL of AO7 and $Fe(SO_4)$ at graphite (●), carbon felt (□), ADE (▲) cathode with a geometric surface of 5 cm^2 at a pH 3. Anode: $Ti/IrO_2–Ta_2O_5$. Experiments performed in conventional cell (in the presence of Na_2SO_4) at 500 A/m^2 and in a micro cell without supporting electrolyte at compact graphite cathode (○) with a nominal distance between the electrodes of 120 μm at 20 A/m^2 at flow rate between 0.05 and 0.1 mL/min. Figure b reports the abatement of TOC of 50 mL of solution in the conventional cell (at compact graphite and carbon felt at 100 A/m^2 and at ADE at 500 A/m^2) and in the microfluidic cell (at compact graphite with an inter-electrode gap of 120 μm, 0.1 ml/min and 60 A/m^2) for a ratio Q/Qth = 4.7.

micro reactor is likely to be due to the ability of micro device to generate high amounts of H_2O_2, thus accelerating the formation of $HO^•$ and consequently the oxidation of organics. Furthermore, in macro cell a supporting electrolyte was necessarily added to the system, thus resulting in the formation of catalytic complexes with ferrous ions with lower catalytic activity [9], while in the microfluidic devices, experiments were carried out in the absence of supporting electrolyte.

To evaluate the effect of iron concentration and current density on the performances of the process, a series of experiments was performed in the micro-fluidic cell with a nominal inter electrode gap of 120 μm by changing both the current density (in the range 10–800 A/m^2) and the concentration of Fe(II). Very similar color and COD removal were achieved at all adopted Fe(II) concentrations (0.25, 0.5, 0.75, 1 mM). According to literature higher abatements were achieved between 20 and 40 A/m^2.

According to the literature, numerous byproducts were detected by HPLC also in this work for the experiments carried out in the conventional cell. The main relevant byproducts were hydroquinone, oxalic and maleic acids (Fig. 7e) which remained in the solution after very long times. When the experiments were repeated in the micro device less byproducts were detected by HPLC (8 and 3 peaks were detected by using the Prevail column under conditions suitable for the evaluation of carboxylic acids, in macro and micro devices, respectively). Regarding the main by-products, maleic acid was present in significantly lower concentrations in the micro device while hydroquinone and oxalic acid were still formed in similar amounts (Fig. 7e). The lower formation of by-products achieved in microreactors could be attributed from one hand to the higher concentrations of hydrogen peroxide achieved in these devices and on the other hand to the absence of supporting electrolyte, thus giving catalytic complexes with higher activity. These factors are likely to enhance the degradation efficacy of EF route, thus giving rise to a more relevant abatement of by-products and allowing the accumulation of significant concentrations only for the more resistant ones.

3.4. Comparison of oxidation routes

Fig. 1 reports the abatement of AO7 (Fig. 1a) and of COD (Fig. 1b) achieved in a conventional cell by the investigated oxidation routes. As shown in Fig. 1a, higher abatement of AO7 was achieved by electro-generated active chlorine with respect to that obtained by EO at both BDD and Iridium based anode. Thus, indirect oxidation routes are not affected by the slow mass transfer of organic pollutant to the anode surface that decreases the performances of the EO process.

On the other hand, a less removal of the COD was observed in the experiments performed with electrogenerated active chlorine with respect to EO at BDD anode (Fig. 1b). Thus, electrogenerated active chlorine is very active for the oxidation of AO7 but not for its mineralization due to the formation of organic intermediates that present a higher resistance to the oxidation by means of active chlorine. Electro-Fenton process gave a very fast but not complete abatement of color. The lower abatement of COD was achieved by EF. This is probably due to the formation of iron complexes of carboxylic acids that are very resistant to the oxidation by means of bulk hydroxyl radicals.

The formation of byproducts was evaluated for all investigated electrocataytic routes by focused HPLC analyses. Oxalic acid was formed in all investigated processes even if in different amounts (see below), maleic acid and hydroquinone in EF and IOAC, formic acid only during EO experiments and lactic and malonic acids only during IOAC ones. Furthermore, a very large number of small peaks was observed by HPLC for the two indirect oxidation processes and in most of cases peaks with different retention times were observed for EF and IOAC. On the other hand for EO at BDD, the chromatograms presented only the peaks attributable to AO7 and oxalic and formic acids. Fig. 7 reports a plot of the concentrations of AO7 and main common byproducts (namely, hydroquinone, oxalic and maleic acid) vs. time for the three investigated electrocatalytic routes. The degradation of AO7 was faster by EO at BDD and slower for EF (Fig. 7a). For EF, a small but not negligible residual concentration of AO7 was observed also after 3 h thus giving rise to a residual coloration of the solution. The lower concentrations of hydroquinone, oxalic and maleic acids were found for EO process. For these compounds, a plot with a maximum was observed for IOAC process. Thus, in the first part of the experiments the generation rate of these compounds is faster than their oxidation rate while the opposite behavior takes place in the second part of the electrolyses an effect of the lower concentration of AO7. On the other hand, for electro-Fenton process, a plot with a maximum was observed for maleic acid while the concentrations of both hydroquinone and oxalic acids still did not decrease also after 3 (Fig. 7) and 24 h (data not shown) of experiments as a result of their higher resistance to oxidation by means of EF.

Fig. 1c and d reports the abatement of AO7 and COD achieved in a micro device. As shown in Fig. 1c, very high abatements of

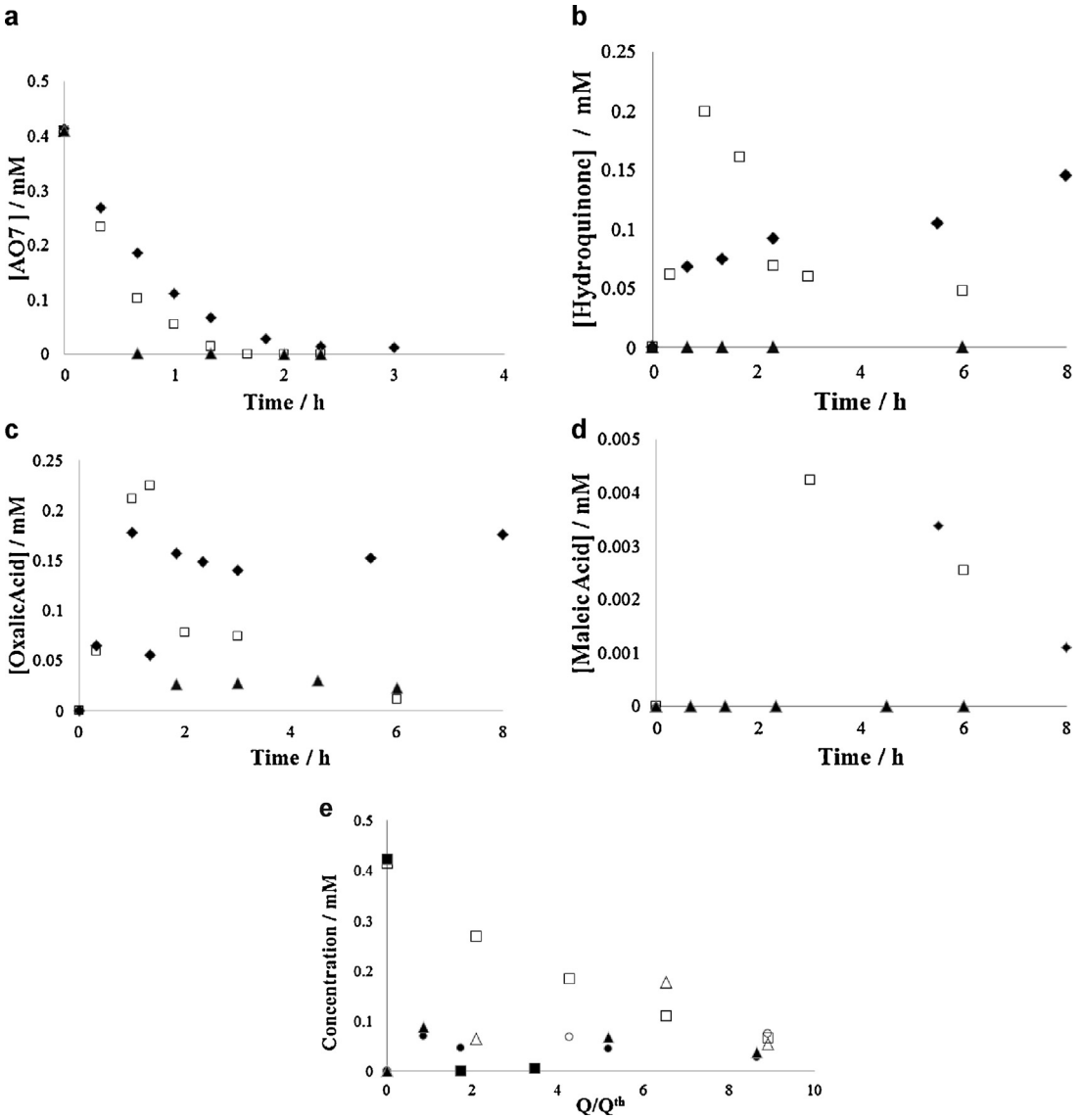

Fig. 7. Time-course of AO7 (a), hydroquinone (b) and oxalic (c) and maleic acids (d) during EO at BDD anode and Ni cathode (▲), EF at compact graphite cathode and Ir based anode with Fe_2SO_4 (♦) and IOAC at Ru based anode and Ni cathode with 17 mM of NaCl (□) in Na_2SO_4 and AO7 (0.4 mM) medium in conventional macro cell at 100 A/m^2. Figure e reports the plot of the concentrations of AO7 (macro (□) and micro (■)), hydroquinone (macro (○) and micro (●)) and oxalic acid (macro (△) and micro (▲)) vs. Q/Q^{th} for the EF process performed with Fe_2SO_4 (0.5 mM) and AO_7 (0.4 mM) at compact graphite cathode and Ir based anode in macro (at 100 A/m^{2}with Na_2SO_4) and micro devices (without supporting electrolyte with a nominal distance between the electrodes 120 μm at flow rate of 0.1 mL/min at a current density of 10–180 A/m^2).

color were achieved by AO at BDD, very close to that obtained by electro-generated active chlorine, as a result of strong intensification of mass transport of the pollutant to the anode surface. Slightly lower abatements were achieved by electro-Fenton process. The higher abatements of COD were obtained at BDD anode also in the micro device (Fig. 1d). On the other hand, very similar abatements of COD were recorded by EF and by means of IOAC, as a result of the dramatic improvement of the performances of EF achieved in the micro device. As above mentioned, this is due to the less formation of byproducts achieved in the microreactor as an effect of high hydrogen peroxide generation and absence of supporting electrolyte.

3.5. Coupled approaches

It has been recently stressed that coupled abatement processes, using both cathode and anode reactions, can allow to enhance significantly the performances of electrochemical approaches in terms of overall abatement of the organic pollutants and current efficiency [21,34]. Fig. 8a reports the abatement of AO7 achieved by electro-Fenton at graphite cathode (with DSA anode and $FeSO_4$ as catalyst), EO at BDD anode (with Ni cathode) and coupled process at BDD anode and graphite cathode with $FeSO_4$ as catalyst. An higher abatement of color was achieved in the coupled process with respect to that observed in both uncoupled processes, for the same amount of charge passed, as a result of the combined action of hydroxyl radicals generated at the BDD anode (BDD–HO$^\bullet$) by the water oxidation and in the bulk of the solution (bulk HO$^\bullet$) by the Fenton process. As shown in Fig. 8b, the adoption of a coupled process involving both EO at BDD and electro-Fenton at graphite gave higher abatements of COD with respect to the sole electro-Fenton but lower than that achieved by EO at BDD with a Nickel cathode. It is known that iron ions form complexes with carboxylic acid that are quite resistant to oxidation. BDD–HO$^\bullet$ are capable to

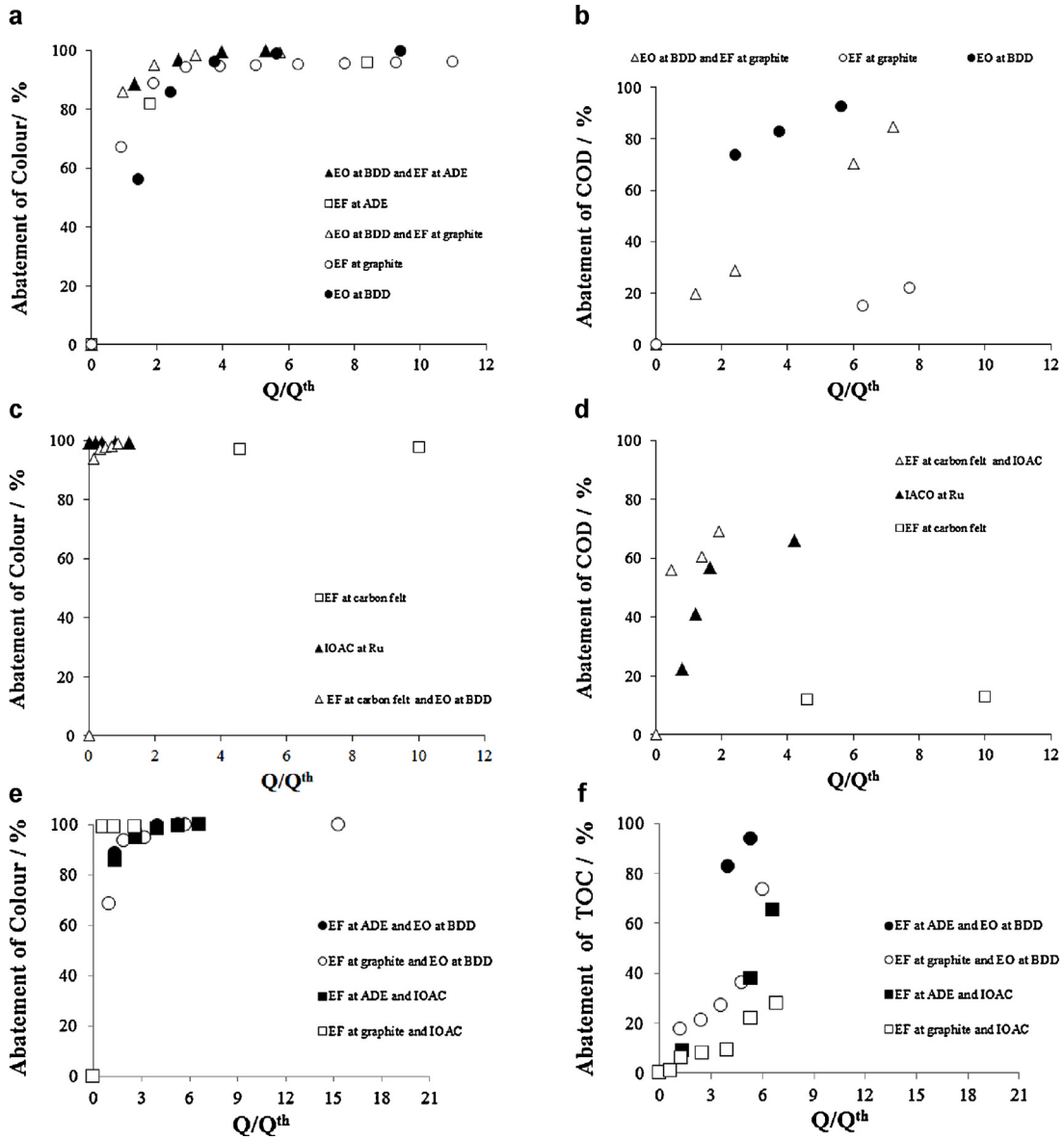

Fig. 8. Comparison between single and coupled processes. Figures a and b report the abatement of colour and COD, respectively, vs. *Q*/*Q*th by EO at BDD (with Ni cathode) (●), electro-Fenton at graphite (○) or ADE (□) cathode with Ti/IrO_2–Ta_2O_5 anode and coupled process at BDD anode and graphite (△) or ADE (▲) cathode. Figures c and d report the abatement of AO7 and COD, respectively, achieved by electro-Fenton at carbon felt cathode with Ti/IrO_2–Ta_2O_5 anode (□), by active chlorine electro-generated at Ru based anode with Ni cathode (▲) and coupled process at Ru based anode and carbon felt cathode (△). A comparison between coupled processes in terms of abatement of AO7 and TOC is reported in Figures e and f. Coupled processes: Electro-Fenton at ADE (●) or graphite (○) cathode and EO at BDD anode, electro-Fenton at ADE (■) or graphite (□) cathode and electro-generation of active chlorine at Ru based anode. Data achieved during the treatment a solution of 50 mL of AO7 in conventional cell (in the presence of Na_2SO_4) at a pH 3 (by addition of H_2SO_4). Experiments at Ru based anode were performed with 17 mM of NaCl. Electrodes with a geometric surface of 3–5 cm^2. Current density: 100 A/m^2.

mineralize also these compounds but longer times are necessary [2]. Very similar results in terms of abatement of color were achieved when the graphite cathode was substituted with an ADE one for both single and coupled process (Fig. 8a). However, as shown in Fig. 8f the abatement of TOC by the coupled process increased drastically in the presence of an ADE cathode.

Fig. 8c and d reports the abatement of color and COD, respectively, achieved by EF at carbon felt cathode (with an iridium based anode and $FeSO_4$ as catalyst), by IOAC at Ru based anode (with Ni cathode and 17 mM of NaCl) and coupled process at Ru based anode and carbon felt cathode (with $FeSO_4$ and 17 mM of NaCl). In this case, the abatement of color was very high with all the processes performed in the presence of electro-generated active chlorine (Fig. 8c) while the abatement of COD was higher for the coupled process (Fig. 8d). Thus, the utilization of a coupled process allows one to use the charge passed at both electrodes to generate oxidants that can react with both AO7 and intermediates formed by the two processes. Furthermore the utilization of NaCl instead of Na_2SO_4 is expected to favor the Fenton process. Indeed, both Cl^- and SO_4^{2-} are regarded as radical scavenger that may retard the oxidation action by means of hydroxyl radicals generated by electro-Fenton process [37]. On the other hand, it is reported that about 80% or 20% of iron (III) is complexed in the presence of 0.05 M sulfate or chlorides, respectively [37,38]. Thus, removal rate of AO7 was reported to be slower in the presence of sulfate ions [9]. On the other hand iron ions form complexes with carboxylic acid that are quite resistant to oxidation and that can adversely affect the oxidation by means of electrogenerated active chlorine.

Fig. 8e and f reports the abatement of color and TOC recorded in tested coupled processes. Very high abatements of color were

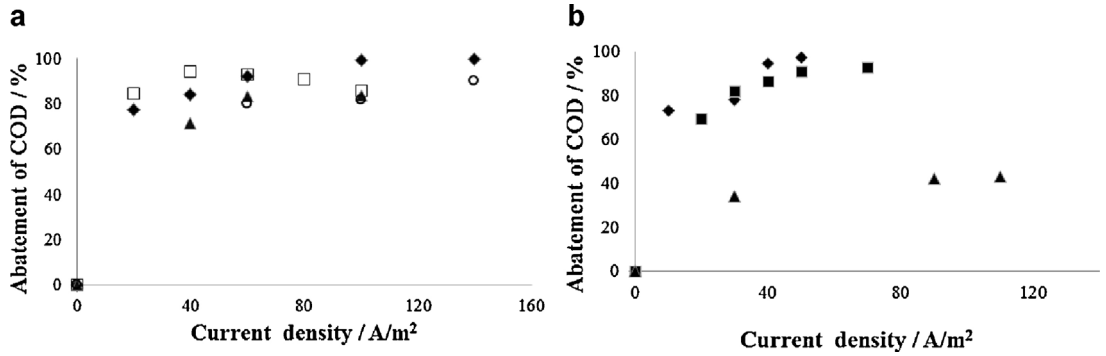

Fig. 9. Comparison between coupled processes. Figure a reports the abatement of COD vs. density current in a micro cell without supporting electrolyte at compact graphite cathode and BDD with a nominal distance between the electrodes of 240 μm (▲), 120 μm (□), 75 μm (○), 50 μm (♦) with a flow rate of 0.1 ml/min at current density between 20 and 140 A/m^2. Figure b reports the abatement of COD vs. current density by EO at BDD anode (with Ni cathode) (■), electro-Fenton at graphite (▲) at Ru based anode and coupled process at BDD anode and graphite (♦) cathode in a micro cell without supporting electrolyte with a nominal distance between the electrodes 50 μm at flow rate of 0.3 mL/min and at density current between 20 and 140 A/m^2. For electro-Fenton and coupled processes, Fe(SO_4) was added to the solution.

achieved by EF-IOAC processes for quite low charge passed (Fig. 8e). On the other hand, EF-EO (at carbon cathodes and BDD anode) gave higher abatement of TOC (Fig. 8f) with respect to coupled processes with electro-generated active chlorine. For both coupled processes higher abatement of TOC were achieved at ADE electrodes.

Coupled EF-EO process was investigated also in microfluidic devices and gave higher abatements of COD with respect to uncoupled processes at all adopted distances between the electrodes, i.e. 50, 120 and 240 μm (see an example data reported in Fig. 9b for an inter-electrodic distance of 50 μm). As shown in Fig. 9a, the performance of EF-EO processes in the micro device strongly depended on the inter-electrodic distance: the higher abatements were achieved at 50 and 120 μm while lower ones were recorded at both 75 and 240 μm. These interesting results are due to the fact that EO benefits from lower inter electrodic distances while EF process gave best results by using an intermediate distance of about 120 μm [13]. As a consequence, when experiments were carried out with an inter electrodic distance of 50 μm, best results were achieved at higher current densities that favor the EO process and, when a spacer of 120 μm was used, higher abatements of COD were obtained by working with the current densities that optimize the EF process (e.g., close to 40 A/m^2).

4. Conclusions

It was shown that the performances of the electrochemical degradation of AO7, in terms of abatement of colour, AO7 and COD and formation of by-products, depend dramatically on the adopted electrocatalytic route:

- Electrochemical treatment with electro-generated active chlorine (IOAC) gave the faster abatement of color.
- The higher abatement rate of COD was achieved by the direct electrochemical oxidation (EO) process at BDD that gave rise to a very small generation of by-products, while the lower one was observed for electro-Fenton (EF) process as a result of the formation of quite resistant by-products that remains in the electrolytic medium also after long electrolysis times.
- Intermediate abatement of COD were given by IOAC as a result of the formation of a number of intermediates that are oxidized with higher rate with respect to EF.

Optimization of investigated catalytic routes occurs under very different operative conditions:

- Performances of IOAC, in terms of abatement of both colour and COD, were improved by working with a Ru based electrode (that gives high generation of active chlorine) and higher current densities and residence times but were not affected by the adopted reactor.
- The performances EO depended obviously on the nature of anode. At BDD anode, higher abatements of both colour and COD were achieved in the microfluidic cell that enhances the mass transport phenomena. Higher abatements of COD but lower current efficiencies were achieved by increasing the current density and lowering the flow rate.
- The abatement of AO7 by electro-Fenton (EF) strongly benefited by the utilization of air diffusion electrode or of a microfluidic reactor. For experiments carried out in the microfluidic reactor, higher abatements of both colour and COD were achieved by working at intermediate values of the current density (between 20 and 40 A/m^2).

Performances of coupled processes (EF-IOAC, EF-EO) were improved using microfluidic devices which furthermore allowed to work in the absence of supporting electrolytes.

Acknowledgment

Università di Palermo is acknowledged for its financial support.

Appendix A. Theoretical model for EO

To rationalize the results achieved by electrochemical direct oxidation of AO7 at BDD a simple model previously proposed by some of authors [22] was used. In the following, the main aspects of the model are briefly summarized.

Main assumptions [22]:

- Constant current electrolyses are considered in the range of potential of oxygen evolution.
- The oxidation of the organics is considered as a surface or a pseudo-surface processes that can take place under oxidation reaction control, mass transfer control or under mixed kinetic regimes depending on the rate of mass transfer of the pollutant toward the anodic surface in comparison with the oxidation rate.
- The chemi-adsorption of the organic pollutant *RH* and of its oxidation products is considered to be negligible.

As a consequence of above mentioned assumptions, the instantaneous current efficiency *ICE* for the treatment of waste waters

contaminated by one organic pollutant can be given by the following expression [22]:

$$ICE = \frac{i_{RH}}{i_{app}} = \frac{i_{RH}}{i_{RH} + i_{O_2}} = \frac{1}{1 + (i_{O_2}/i_{RH})} = \frac{1}{1 + ([RH]^*/[RH]^{y=0})} \quad (18)$$

where i_{RH} and i_{O_2} are the current densities involved in the oxidation of the organic and in the oxygen evolution process, respectively, i_{app} is the applied current density, $[RH]^{y=0}$ is the concentration of the organic *RH* at the anodic surface and the term $[RH]^*$ is the value of $[RH]^{y=0}$ which gives a current density for the *RH* oxidation equal to the current density involved for the oxygen evolution reaction, e.g. the value of $[RH]^{y=0}$ that gives a current efficiency of 50%.

Under pseudo-steady state conditions, prevailing during an electrolysis carried out with amperostatic alimentation, the following expression should apply:

$$k_m([RH]^b - [RH]^{y=0}) = \frac{i_{app}\, ICE}{nF} \quad (19)$$

where k_m is the mass transfer constant and $[RH]^b$ is the concentration of the organic in the bulk of the aqueous phase. Hence, by combination of Eqs. (18) and (19) and elimination of the term $[RH]^{y=0}$, one can obtain the expression for the *ICE* reported in Eq. (20).

$$ICE = \frac{1}{1 + \left(2[RH]^* / \left([RH]' + \left([RH]'^2 + 4[RH]^*[RH]^b\right)^{0.5}\right)\right)} \quad (20)$$

where $[RH]' = [RH]^b - [RH]^* - C^*$, $C^* = i_{app}/(nFk_m)$, n is the number of electrons exchanged for the anodic oxidation of *RH* to carbon dioxide or to a stable product, F the Faraday constant (96,487 C mol^{-1}).

In the limiting cases of an organic concentration, respectively, strongly higher and strongly lower than $C^* = i_{app}/(nFk_m)$ the following expressions can be furthermore considered [22].

- Oxidation reaction control ($i_{lim} = nFk_m[RH]^b \gg i_{app} ICE^{OC}$ (i.e., if $[RH]^b \gg C^* ICE^{OC}$)

$$ICE^{OC} = \frac{1}{1 + ([RH]^*/[RH]^b)}$$

- Mass transfer control ($i_{lim} \ll i_{app} ICE^{OC}$ (i.e., $[RH]^b \ll C^* ICE^{OC} < C^*$))

$$ICE^{MT} \approx \frac{[RH]^b}{C*} = \frac{nFk_m[RH]^b}{i_{app}}$$

References

[1] T. Robinson, G. McMullan, R. Marchant, P. Nigam, Bioresour. Technol. 77 (2001) 247–255.
[2] C.A. Martínez-Huitle, E. Brillas, Appl. Catal. B: Environ. 87 (2009) 105–145.
[3] E. Forgacs, T. Cserhati, G. Oros, Environ. Int. 30 (2004) 953–971;
G.M. Atenas, E. Mielczarski, J.A. Mielczarski, J. Colloid Interface Sci. 289 (2005) 171–183.
[4] A. Fernandes, A. Morao, M. Magrinho, A. Lopes, I. Goncalves, Dyes Pigments 61 (2004) 287–296.
[5] W.L. Chou, C.T. Wang, C.P. Chang, Desalination 266 (2011) 201–207.
[6] C. Zhang, J. Wang, T. Murakami, J. Electroanal. Chem. 638 (2010) 91–99.
[7] J.M. Peralta-Hernandez, Y. Meas-Vong, F.J. Rodríguez, T.W. Chapman, M.I. Maldonado, L.A. Godínez, Dyes Pigments 76 (2008) 656–662.
[8] A. Ozcan, M.A. Oturan, N. Oturan, Y. Sahin, J. Hazard. Mater. 163 (2009) 1213–1220;
S. Hammami, N. Bellakhal, N. Oturan, M.A. Oturan, M. Dachraoui, Chemosphere 73 (2008) 678–684.
[9] N. Daneshvar, S. Aber, V. Vatanpour, M.H. Rasoulifard, J. Electroanal. Chem. 615 (2008) 165–174.
[10] S. Garcia-Segura, F. Centellas, C. Arias, J.A. Garrido, R.M. Rodriguez, P.L. Cabot, E. Brillas, Electrochim. Acta 58 (2011) 303–311.
[11] O. Scialdone, C. Guarisco, A. Galia, G. Filardo, G. Silvestri, C. Amatore, C. Sella, L. Thouin, J. Electroanal. Chem. 638 (2010) 293.
[12] O. Scialdone, A. Galia, C. Guarisco, Electrochim. Acta 58 (2011) 463–473.
[13] O. Scialdone, A. Galia, S. Sabatino, Electrochem. Commun. 26 (2013) 45–47.
[14] P. He, P. Watts, F. Marken, S.J. Haswell, Electrochem. Commun. 7 (2005) 918–924.
[15] J.M. Aquino, G.F. Pereira, R.C. Rocha-Filho, N. Bocchi, S.R. Biaggio, J. Hazard. Mater. 192 (2011) 1275–1282.
[16] C.A. Martinez-Huitle, S. Ferro, A. De Battisti, J. Appl. Electrochem. 35 (2005) 1087–1093.
[17] P. Cañizares, R. Paz, C. Saez, M.A. Rodrigo, J. Environ. Manage. 90 (2009) 410.
[18] C.A. Martinez-Huitle, S. Ferro, Chem. Soc. Rev. 35 (2006) 1324–1340.
[19] O. Scialdone, A. Galia, G. Filardo, Eletrochim. Acta 53 (2008) 7220–7225.
[20] M. Panizza, G. Cerisola, Electrochim. Acta 51 (2005) 191–199.
[21] O. Scialdone, A. Galia, C. Guarisco, S. La Mantia, Chem. Eng. J. 189–190 (2012) 229–236.
[22] O. Scialdone, Electrochim. Acta 54 (2009) 6140–6147;
O. Scialdone, A. Galia, S. Randazzo, Chem. Eng. J. 183 (2012) 124–134.
[23] C. Comninellis, Electrochim. Acta 39 (1994) 1857–1862.
[24] O. Scialdone, S. Randazzo, A. Galia, G. Silvestri, Water Res. 43 (2009) 2260–2272.
[25] L. Szpyrkowicz, J. Naumaczky, F. Zilio-Grandi, Toxicol. Environ. Chem. 44 (1994) 189–202.
[26] C.H. Yang, C.C. Lee, T.C. Wen, J. Appl. Electrochem. 30 (2000) 1043–1051.
[27] L.C. Chiang, J.E. Chang, T.C. Wen, Water Res. 29 (1995) 671–678.
[28] Ch. Comninellis, A. Nerini, J. Appl. Electrochem. 25 (1995) 23–28.
[29] F. Bonfatti, S. Ferro, F. Lavezzo, M. Malacarne, G. Lodi, A. De Battisti, J. Electrochem. Soc. 147 (2000) 592–596.
[30] C.A. Martinez-Huitle, S. Ferro, A. De Battisti, Electrochem. Solid-State Lett. 11 (2005) D35–D39.
[31] A. Sánchez-Carretero, C. Sáez, P. Cañizares, M.A. Rodrigo, Chem. Eng. J. 166 (2011) 710–714.
[32] A.M. Polcaro, A. Vacca, M. Mascia, S. Palmas, J. Rodriguez Ruiz, J. Appl. Electrochem. 39 (2009) 2083–2092.
[33] M.E.H. Bergmann, J. Rollin, T. Iourtchouk, Electrochim. Acta 54 (2009) 2102–2107.
[34] E. Brillas, I. Sires, M.A. Oturan, Chem. Rev. 109 (2009) 6570.
[35] J.S. Do, C.P. Chen, J. Electrochem. Soc. 140 (1993) 1632.
[36] A. Da Pozzo, L. Di Palma, C. Merli, E. Petruccci, J. Appl. Electrochem. 35 (2005) 413–419.
[37] J. De Laat, G.T. Le, B. Legube, Chemosphere 55 (2004) 715–723.
[38] O. Scialdone, A. Galia, S. Randazzo, Chem. Eng. J. 174 (2011) 266–274.
[39] N. Oturan, J. Wu, H. Zhang, V.K. Sharma, M.A. Oturan, Appl. Catal. B: Environ. 140–141 (2013) 92–97.
[40] I. Sirés, J.A. Garrido, R.M. Rodríguez, E. Brillas, N. Oturan, M.A. Oturan, Appl. Catal. B: Environ. 72 (2007) 382–394.